Journal of Structural Biology: X 6 (2022) 100057

Contents lists available at ScienceDirect

Journal of Structural Biology: X

journal homepage: www.sciencedirect.com/journal/journal-of-structural-biology-x

Graphical Structural Biology Review

Hierarchical organization of bone in three dimensions: A twist of twists

Daniel J. Buss [a], Roland Kröger [b], Marc D. McKee [a,c], Natalie Reznikov [d,*]

[a] Department of Anatomy and Cell Biology, McGill University, 3640 University Street, Montreal, Quebec H3A 0C7, Canada
[b] Department of Physics, University of York, Heslington, York YO10 5DD, United Kingdom
[c] Faculty of Dentistry, McGill University, 3640 University Street, Montreal, Quebec H3A 0C7, Canada
[d] Department of Bioengineering, McGill University, 3480 University Street, Montreal, Quebec H3A 0E9, Canada

ARTICLE INFO

Keywords:
Bone
Biomineralization
Volume Microscopy and Tomography
Electron Microscopy
Hierarchical Organization
Helicoidal Structures
Skeleton
Review

ABSTRACT

Structural hierarchy of bone – observed across multiple scales and in three dimensions (3D) – is essential to its mechanical performance. While the mineralized extracellular matrix of bone consists predominantly of carbonate-substituted hydroxyapatite, type I collagen fibrils, water, and noncollagenous organic constituents (mainly proteins and small proteoglycans), it is largely the 3D arrangement of these inorganic and organic constituents at each length scale that endow bone with its exceptional mechanical properties. Focusing on recent volumetric imaging studies of bone at each of these scales – from the level of individual mineralized collagen fibrils to that of whole bones – this graphical review builds upon and re-emphasizes the original work of James Bell Pettigrew and D'Arcy Thompson who first described the ubiquity of spiral structure in Nature. Here we illustrate and discuss the omnipresence of twisted, curved, sinusoidal, coiled, spiraling, and braided motifs in bone in at least nine of its twelve hierarchical levels – a visualization undertaking that has not been possible until recently with advances in 3D imaging technologies (previous 2D imaging does not provide this information). From this perspective, we hypothesize that the twisting motif occurring across each hierarchical level of bone is directly linked to enhancement of function, rather than being simply an energetically favorable way to assemble mineralized matrix components. We propose that attentive consideration of twists in bone and the skeleton at different scales will likely develop, and will enhance our understanding of structure–function relationships in bone.

Introduction

Ingenious structural arrangements found at every scale throughout Nature permit the wide range of functions that organisms rely on for movement, feeding, protection, and reproduction. In the vertebrate skeleton, hierarchical organization of the primary organic (type I collagen) and inorganic mineral (carbonate-substituted hydroxyapatite) constituents determines a balance between the stiffness and toughness of this lightweight framework. This allows vertebrates to move against gravitational forces, and provides protection against mechanical impacts, all at a reasonable metabolic cost. Following from over a century of structural studies on bone, and now supported by recent investigations aided by the development of 3D volume electron microscopy and deep learning-aided segmentation methods, this graphical review highlights the presence of twisted, curved, sinusoidal, coiled, spiraling and braided motifs in at least nine of the hierarchical levels in bone (out of about twelve known to date). Having been inspired by the spiraling of fibers found in his original dissections of heart tissue, James Bell Pettigrew emphasized the ubiquity of the spiral in Nature and hypothesized its relation to function (Gardner, 2017; Pettigrew, 1908). His colleague D'Arcy Thompson comprehensively described the importance of spirals in biological objects (Thompson, 1942). He emphasized that the spiral is a common and generic shape used in many instances of biology, with just graded change in the radius of curvature resulting in geometric differences ranging between (for example) the subtly arced horns of the Oryx to the coiling tendrils of creeping plants. From these observations, we extend Pettigrew's and Thompson's thinking on spirals and twists to various additional hierarchical arrangements of structure in the vertebrate skeleton enabled by new visualization methods.

From the speedy cheetah that coils and uncoils her entire body in each stride, to the tiny hovering hummingbird that sketches a distinct "figure eight" shape with every wing stroke (Stolpe and Zimmer, 1939), macroscopic twisting and curving of skeletal assemblies are key to function. Although these are kinematic observations, even in a static

* Corresponding author.
E-mail address: natalie.reznikov@mcgill.ca (N. Reznikov).

https://doi.org/10.1016/j.yjsbx.2021.100057
Received 14 September 2021; Received in revised form 3 December 2021; Accepted 6 December 2021
Available online 9 December 2021

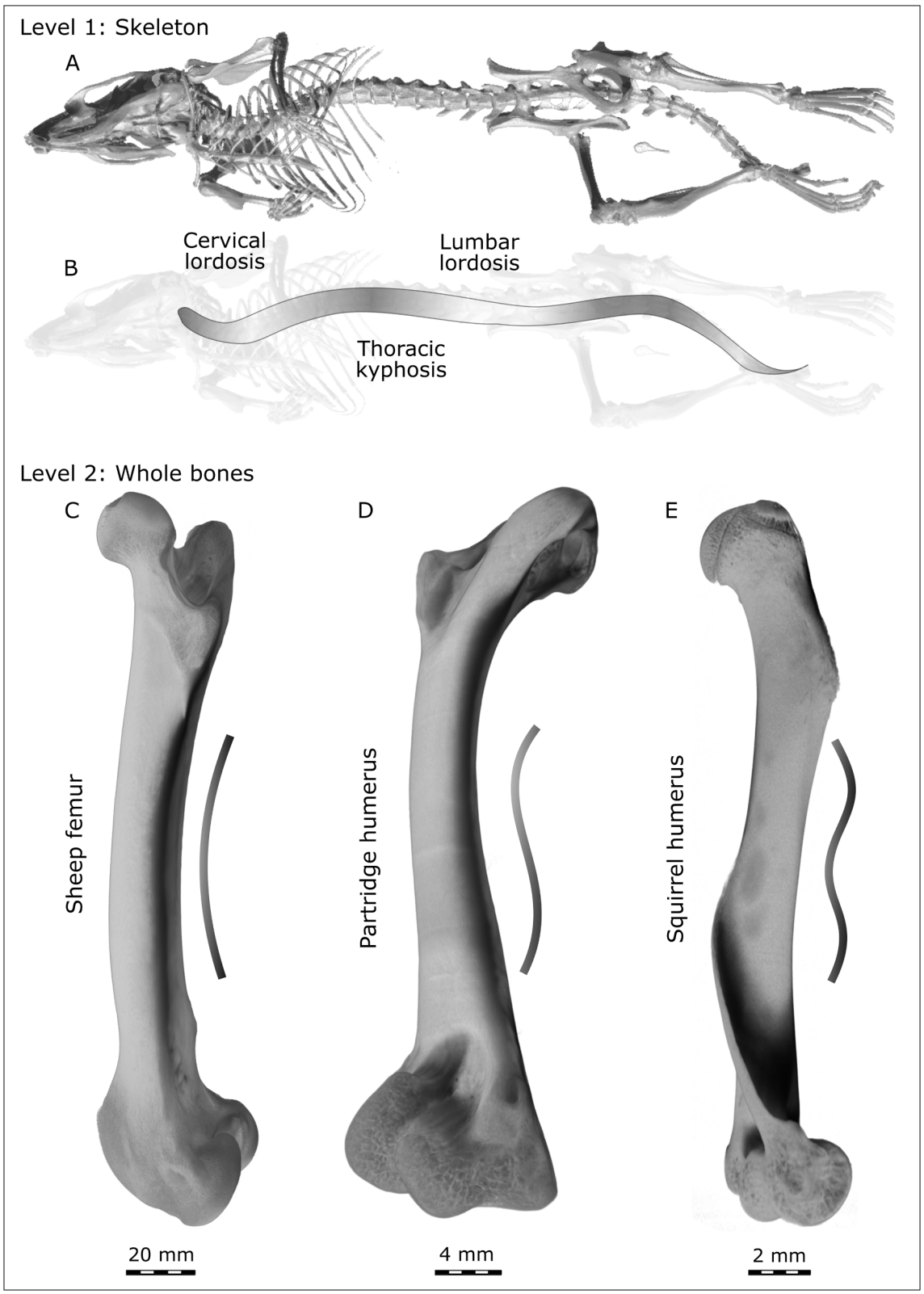

Fig. 1. Hierarchical levels of the full skeleton and of whole bones. (A,B) A mouse skeleton imaged using microcomputed tomography (μCT). The same structural plan can be observed in the skeletons of mammals: here, the murine spine shows the same principle curves as the human spine – cervical and lumbar lordosis (convexity oriented forwards) and thoracic kyphosis (concavity oriented forwards). (C, D, E) Individual bones (imaged by μCT) scaled to the same figure height: sheep femur (C) with its shallow c-shaped curvature, partridge humerus (D) with an s-shaped curvature, and squirrel humerus (E) showing a screw-shape geometry.

view obvious curvatures can be commonly seen in vertebrates, for example, along the length of the spine. Expectedly, given the fact that most quadrupedal animals share the same body plan, a similar curvature can be found in many spines (as shown in the mouse skeleton in Fig. 1A, B). At the level of individual bones, twisting may be observed when one dimension exceeds another. Our ribs follow a screw trajectory around

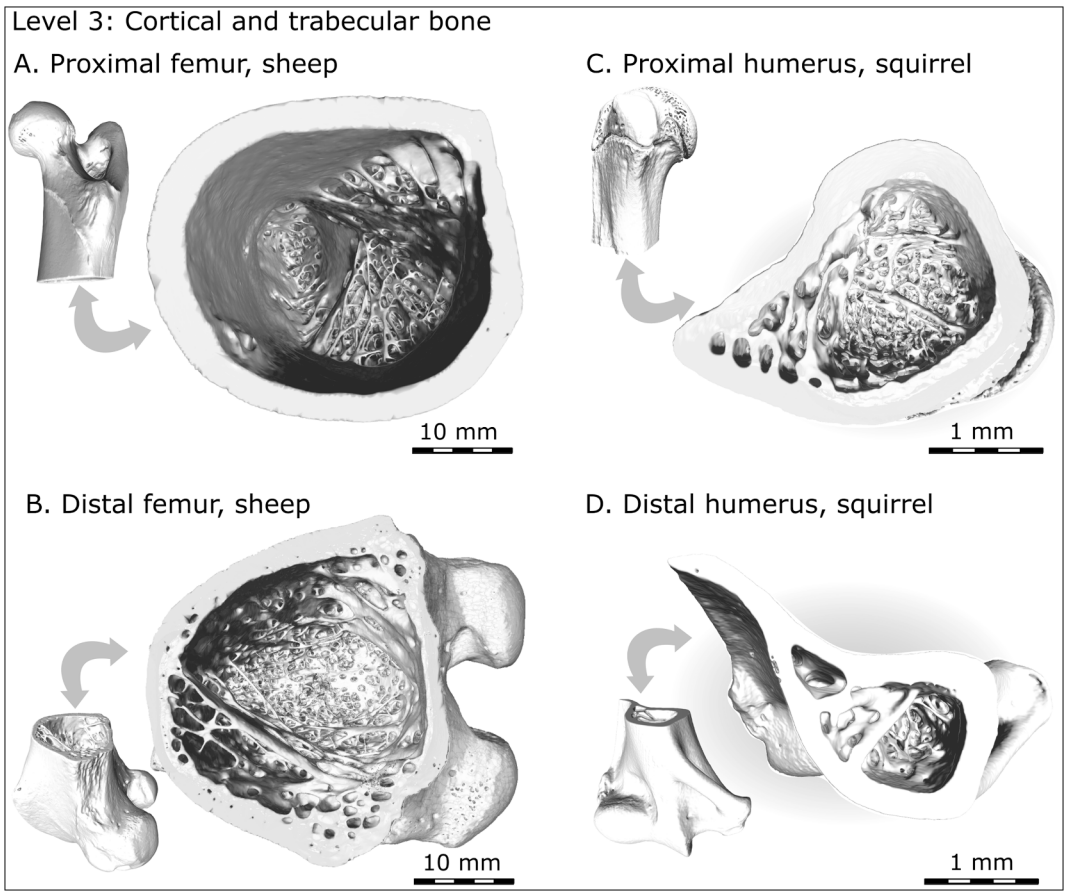

Fig. 2. Cortical-to-trabecular bone transition (hierarchical Level 3) in the metaphyses of the sheep femur (A, B) and the squirrel humerus (C, D). Note that both proximal metaphyses show geometric "vorticity" of trabecular buttresses (A, C), but this is not that obvious in the distal metaphyses (B, D).

the body axis, and our clavicles are twisted around their own axes (Cook, 1914). In short bones, such as vertebrae or metacarpals, it is naturally difficult to observe overt twisting at this level. While a gentle curvature and twist typically can be seen in most long bones (Fig. 1C and 1D), in some species such as squirrels this twist is quite pronounced (Fig. 1E). In fact, the degree of twisting in humeri among ancient fossil mammals appears to be indicative of overall preferred posture attributed to a particular species (Gambaryan and Kielan-Jaworowska, 1997), therefore reflecting the biomechanical environment of an organism.

At a higher magnification level (millimeter scale), where cortical bone can be distinguished from trabecular bone, twisting may not be immediately apparent. The epiphyses and metaphyses of long bones are characterized by a 3D network of plate and rod-like trabeculae within a cortical shell. Nearing the transition from metaphysis to diaphysis, trabeculae form fine and then coarse struts that fuse into larger buttresses. However, observation of this transition from the axial aspect (Fig. 2) reveals a twisting staircase-like structure as trabecular struts seem to spiral around the bone's central axis. Interestingly, this twisting appears to be more pronounced at the proximal metaphyses of the femur and humerus, where the range of movement is broadest. This level is the last one at which an overall curvature, or spiral, or twist, can be observed by an unaided eye – for the higher magnification levels, digital image analysis methods are employed.

The next level of spiraling is that of the osteons which surround the osteonal (Haversian) canal system in the cortical bone of large animals. It is technically challenging to visualize osteonal canals in 3D (usually done with micro-computed tomography, μCT) over an entire bone specimen. In small animals like laboratory rodents, there is minimal osteonal remodeling (therefore, scarce osteonal canals to image). In large animals like pig or sheep, who do undergo osteonal remodeling, the larger bone sizes typically prohibit imaging with resolution high enough to resolve the canals of 40–50 μm in diameter, unless scanning of a long bone is done in portions that are digitally "stitched" together. Incomplete osteons, in which concentric lamellae are in the process of being deposited, have a wider lumen, up to a few hundred micrometers. Fig. 3A shows the resorption canals and incomplete osteons in the femur of a juvenile sheep where these cavities are about 100 μm wide and therefore can be imaged with micro-computed tomography and then segmented over the entire specimen. Fig. 3B shows the far less numerous resorption canals and incompletely filled osteons in a mature sheep femur. From this, spiraling is indeed observed around the shaft axis with a pitch of about 5-15°. This corroborates the work by Hert et al. (Heřt et al., 1994), although their study was not in 3D (Fig. 3C), in which ground sections of human bone dyed with India ink were found to have a similar low-pitch twist, with symmetry between right and left limbs. Functionally, the helicoid trajectory of the capillary-containing canals along a bone shaft likely mitigates the stress-raising effect of local discontinuities that are present in bone at many structural levels (Currey, 2003; Currey and Shahar, 2013).

The next hierarchical level in bone architecture is the wrapping of concentric lamellar layers around the osteonal canals. Wagermaier *et al.* in 2006 using micro-beam wide-angle X-ray scattering showed that the pitch of multiple lamellar layers of the same osteon varies cyclically between having a low angle and a high angle (Wagermaier et al., 2006) (Fig. 3D). Of interest, they observed that the angle was never 0° nor 90°, and that the handedness of lamellar layers was the same, except for a few outermost lamellar layers. Thus, an osteon can be viewed as an assembly of concentric nested springs/coils that provide for better mechanical resilience: "Helicoidal structures have certain advantages in resisting mechanical loads compared to orthogonal plywood structures since the

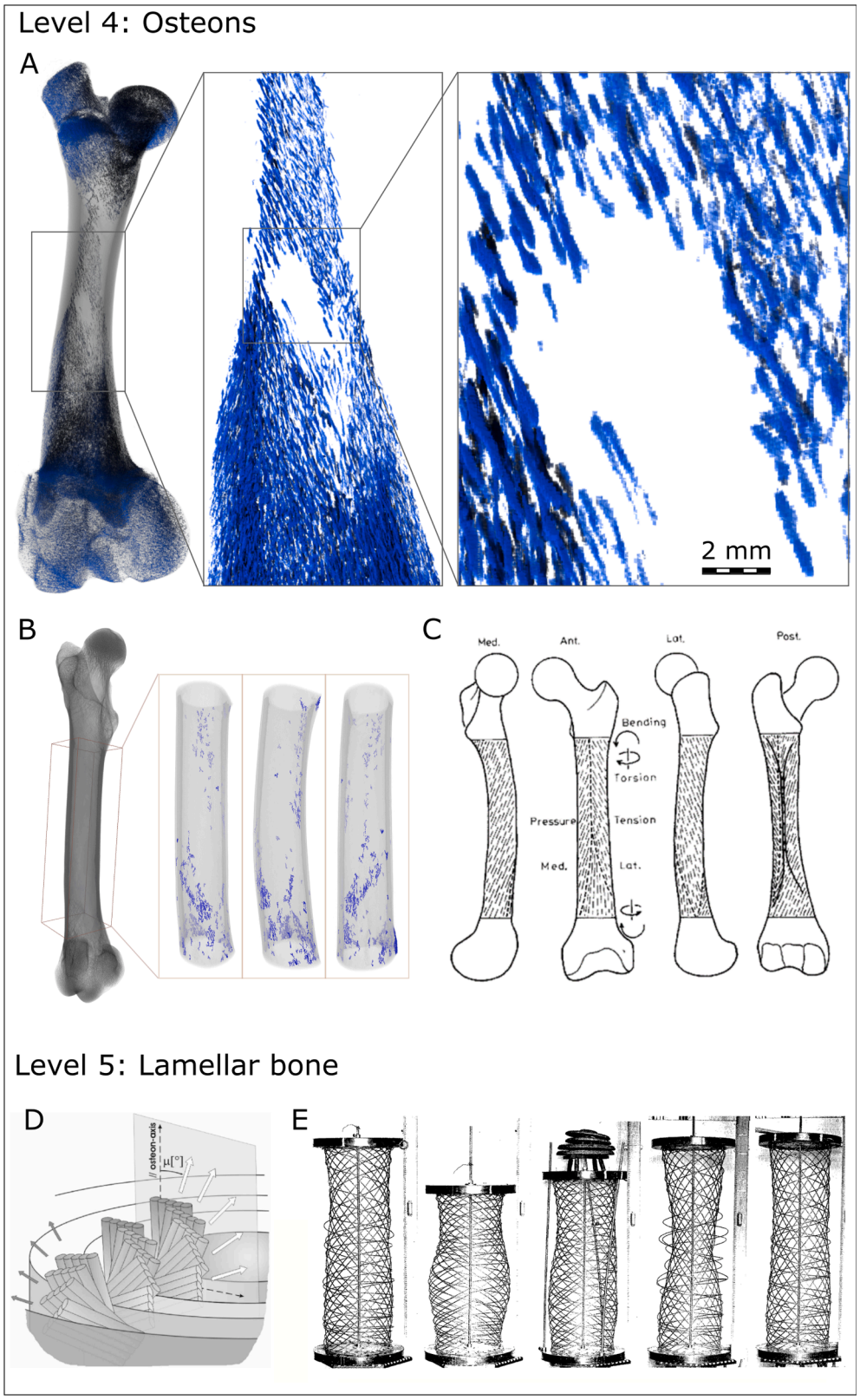

Fig. 3. Vascular canals in a sheep femur (hierarchical Level 4), and winding of lamellar layers around the canals (osteons, hierarchical Level 5). (A) Resorption cavities and incomplete osteons within a juvenile sheep. (B) Less-abundant resorption canals and incomplete osteons in a mature sheep femur. Note the similarity between B and the "hatching" of osteonal canals in the human femur (from Hert et al. (Heřt et al., 1994) , with permission). (D) Spiral winding of co-oriented mineralized collagen fibrils around the central capillary of an osteon, from Wagermaier et al. (Wagermaier et al., 2006), with permission. The lamellar assembly in the whole osteon can be viewed as a series of concentric nested coils. Note the switch in handedness in the outermost layer. (E) Preceding work by Gebhardt (Gebhardt, 1906) in 1906, who empirically illustrated the stiffening effect of multi-layered coiling assemblies with varying pitch and handedness: either in tension, compression or torsion, there will always be a subset of lamellae that resist such deformation axially.

twisted orientation enables a higher extensibility in tension and compression" (Wagermaier et al., 2006). However, already a hundred years prior, Gebhardt (Gebhardt, 1906) in his seminal work on osteonal structure explained the importance of alternating pitch and alternating handedness to resist torsional deformation and buckling (Fig. 3E). It is of interest to note that circumferential lamellar layers display a similar range of pitch angles with respect to the long bone axis (Reznikov et al., 2013).

To properly resolve and assess structures beyond the aforementioned levels, covering now the micro- and nanoscales, electron microscopy is typically employed. One particular method which has provided for significant advances in understanding bone's hierarchical organization

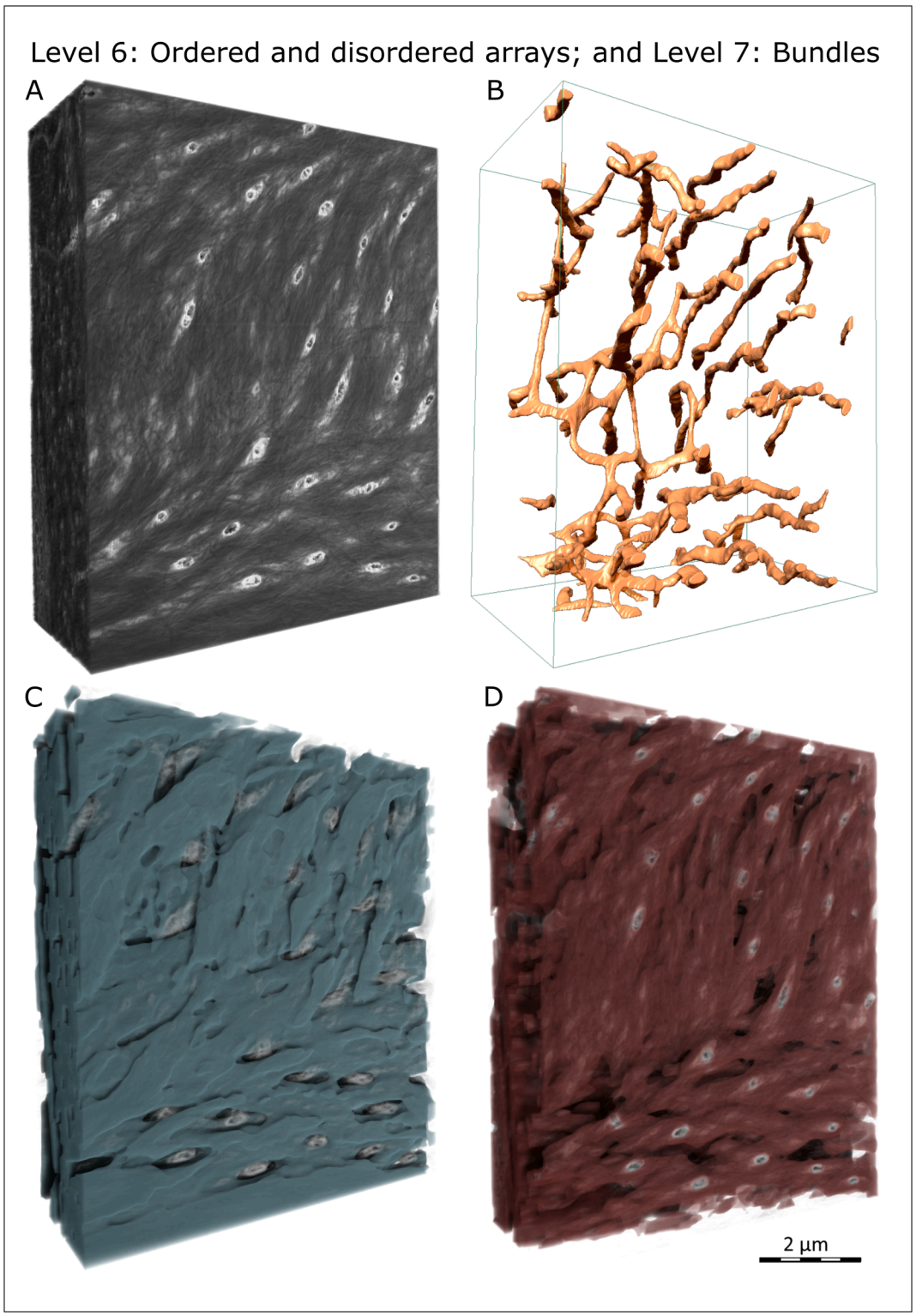

Fig. 4. Hierarchical Level 6 (ordered and disordered repeats in the lamellar structure), and Level 7 (packing of co-aligned collagen fibrils into quasi-cylindrical bundles). These images were acquired using the FIB-SEM slice-and-view method on demineralized and stained lamellar bone. (A) Grey-scale 3D volume in which collagen fibrils appear dark grey, interfibrillar ground matter appears light grey, the *lamina limitans* lining canaliculi is white, and osteocyte processes are also white. (B) The same canaliculi as in A, surface-rendered and shaded to illustrate their meandering course across the ordered bundles, and their screw-shaped axial twist. (C) Segmentation of the ordered arrays of collagen, 3D rendered and superimposed on a semi-transparent grey-scale volume (same sample and same orientation as in A). Note the braided and gently twisted appearance of splitting and merging bundles of collagen fibrils. (D) Disordered collagen fibrils alternate with the ordered bundles and house the cellular processes. Here, the disordered phase has been segmented using deep learning-aided segmentation, and its content is about 30% with respect to the total volume of the extracellular matrix (original nonquantitative work by Reznikov *et al.* (Reznikov et al., 2013) underestimated the proportion of the disordered array by volume).

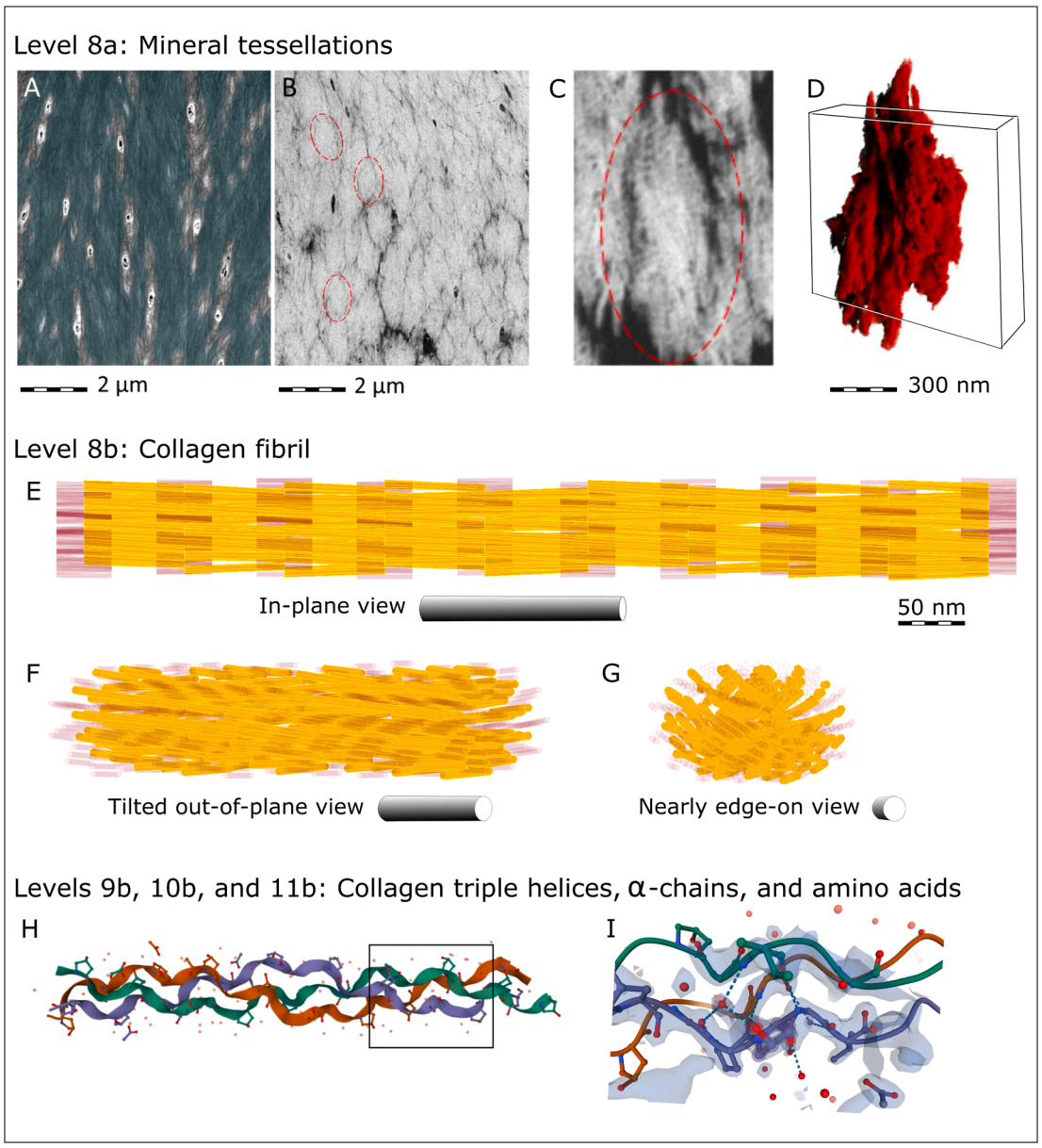

Fig. 5. Hierarchical Level 8a – prolate ellipsoidal mineral tessellations that populate bundles of ordered collagen fibrils in lamellar bone. (A) 2D view from Fig. 4A and 4C. (B) An orientation- and magnification-matched 2D view of undemineralized bone from Buss *et al.* (Buss et al., 2020). (C) A further magnified 2D image of a typical mineral aggregate – a "tesselle". (D) A 3D rendering of a typical single tesselle, as outlined by dashed red ellipses in panels B and C (the tesselle in panel C is one 2D cross-sectional view of its subsequent 3D volume shown in panel D). The rectangular box in panel C roughly corresponds to the complete volume of interest presented in the following Fig. 6. (E) Hierarchical Level 8b showing a supertwisted model of a mineralized collagen fibril with a characteristic stagger of triple helices and a 5° molecular tilt with respect to the fibril axis, reminiscent of the seed arrangement in the sunflower, as suggested by Charvolin and Sadoc (Charvolin and Sadoc, 2011, 2012). Gap regions between collagen triple helices are depicted in transparent red with the hydroxyapatite crystals represented in yellow. (F, G) The same 3D supertwisted collagen model rotated around the vertical axis ("yaw") to accentuate the resultant spiraling alignment of the gaps and the mineral crystallites that would be confined to the gap zones. Panels H and I show the hierarchical structure of collagen only at the levels of triple helices, α-chains and amino acids (images adapted from the RCSB Protein Data Bank (Bella et al., 1994; Kramer et al., 1998; Sehnal, 2021); https://doi.org/10.2210/pdb1CAG/pdb). The corresponding organizational levels for bone mineral are shown in Figs. 6 and 7.

over the past ten years or so has been serial-surface-view (also called slice-and-view) imaging using the focused-ion beam scanning electron microscope (FIB-SEM). This method uses sequential electron imaging and ion beam milling (typically gallium ions) to produce a stack of 2D images that are reconstructed into a 3D volume of nanometer-scale voxel resolution. Using this approach, the Weiner lab was the first to comprehensively characterize the 3D sub-lamellar organization of collagen in decalcified lamellar bone (Reznikov et al., 2013; Reznikov et al., 2014a; Reznikov et al., 2014b; Reznikov et al., 2015). They showed that lamellar alignment is also never strictly along or across the osteonal axis, with the winding angle varying between 15 and 80°. They also illustrated a previously unidentified level of hierarchical organization, these being "order" and "disorder" as repeating components of the lamellar sequence. The lacuno-canalicular network – housing osteocyte cells and their dendritic cell processes – is contained entirely within the disordered collagen array (Reznikov et al., 2013; Reznikov et al., 2014a). The canaliculi with their resident cell processes meander across repetitive lamellar layers, at the same time displaying a screw-like twist (Fig. 4B), which is in accord with the biomechanical incentive to minimize the stress-concentrating factor (Currey and Shahar, 2013). It

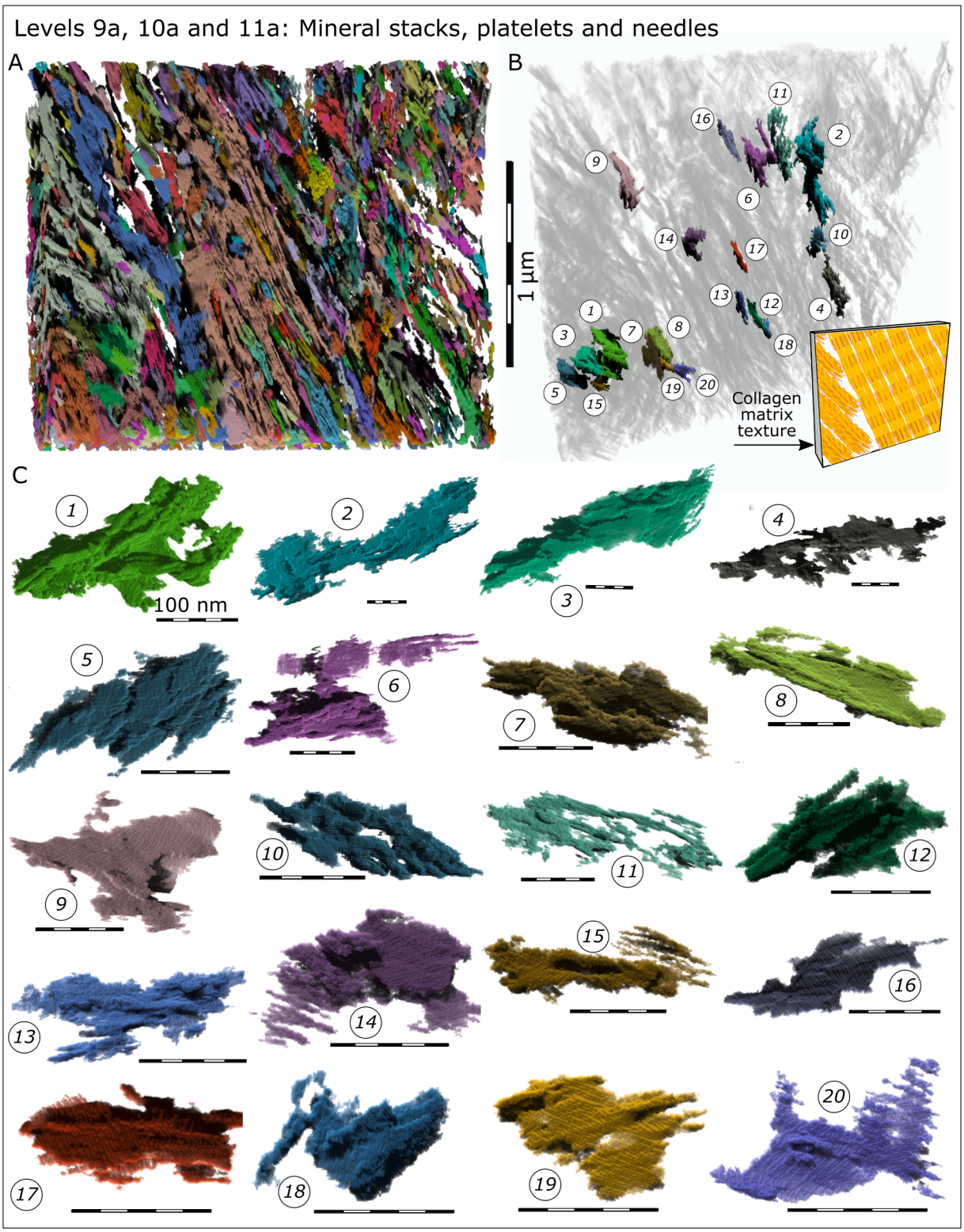

Fig. 6. Hierarchical Levels 9, 10 and 11 of bone mineral organization: stacks, plates and needles. (A) STEM tomography of a FIB-milled foil of lamellar bone. The contrast originates from the crystallites' electron density, and all the crystallites are segmented (using a deep neural network), volume-rendered, and color-coded following a watershed transformation. (B) Twenty digitally separable crystallite aggregates are shown *in situ* (in unmodified orientations) within the same STEM tomographic volume as in A. The remaining tomogram volume is rendered transparent. The yellow inset in the bottom right corner of panel B schematically illustrates the orientation of collagen fibrils within the tomogram rendered in panels A and B. (C) A gallery of 20 digitally separable crystallite aggregates ranging in size between 10^6 nm^3 and 10^5 nm^3 (in a descending order). Individual aggregates are intentionally shown in re-orientations different from those orientations observed *in situ*.

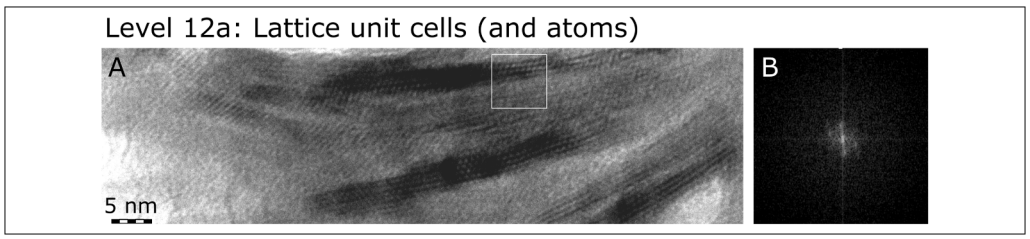

Fig. 7. Hierarchical Level 12, here pertaining only to the mineral component of bone, is represented by the unit cells and atoms themselves comprising bone mineral crystallites (A). Panel B shows a Fourier transform of the area outlined in (A) by the white square.

remains to be seen if there is a discernable twist of the actual osteocyte dendrites on a larger scale (Buss et al., 2020; Hasegawa et al., 2018) – indeed undoubtedly an elusive question to answer, given the need for such high resolution over a large volume of interest. An additional observation at this level of hierarchy is that the layers of ordered collagen matrix are not discontinuous entities; they form bundles of 1–3 μm in diameter that are quasi-cylindrical in shape, splitting and merging continuously, and twisting around their own axes (Reznikov et al., 2014a; Reznikov et al., 2014b). Collectively, these 3D FIB-SEM tomography works confirmed earlier SEM observations of collagen bundles by Boyde and Hobdell (Boyde and Hobdell, 1968) (Fig. 4C, D). Segmentation of twisted and braided bundles of collagen in 3D reconstructions as shown in hierarchical Level 7, which comprise the ordered collagen array, was then made possible a few years later with the arrival of deep learning applied to this type of bioimaging (Reznikov et al., 2020).

More recent studies using serial-surface-view FIB-SEM imaging on mineralized (not demineralized) bone specimens has revealed a subtle twisting that takes place at the next hierarchical level, at the level of crossfibrillar mineral tessellation (Ayoubi et al., 2021; Binkley et al., 2020; Buss et al., 2020). These micron-sized mineral "tesselles" are generally observed as abutting polycrystalline mineral aggregates whose morphology geometrically approximates prolate ellipsoids whose longer axis generally follows the direction of collagen fibrils (McKee et al., 2021). Thus, across the microscale, this tessellated arrangement of mineral that traverses and bridges collagen fibrils in a crossfibrillar manner presumably acts as a toughening mechanism, resisting compression, and perhaps acting as a sublamellar mechanism for crack deflection. Fig. 5A shows ordered arrays of segmented collagen bundles at the micrometer level, merging and twisting (demineralized for visibility) and size-wise what would be a matching field-of-view of undemineralized bone (Fig. 5B) showing the interlocking, abutting mineral tessellations within mature mineralized lamellar bone. The space-filling assembly of rigid abutting tesselles within a continuous viscous collagenous matrix, so that the many narrow 3D interfaces remain unfused, may contribute to reconciling the conflicting properties of stiffness and toughness in bone (Buss et al., 2020). A single tesselle from a human femur (Fig. 5C) is rendered in 3D (Fig. 5D): note the spindle-shape and twist at this structural level which mimics and contributes to the larger overall twist at the collagen bundle level where many tesselles pack together. This particular tesselle was imaged at the near-limit of FIB-SEM resolution using a voxel size of 4 nm, and it was labeled using deep learning-based segmentation (Dragonfly™, Object Research Systems Inc., Montreal).

At finer size scales, the organization of collagen itself has been extensively documented (using a variety of methods) as twisted superhelical arrays, all the way down to the level of amino acids of individual alpha chains, to the coiling of these chains into the triple helix of collagen molecules, and even to the slight twisting of molecules within the fibril itself (Bella et al., 1994; Charvolin and Sadoc, 2011, 2012; Giraud-Guille, 1992; Kramer et al., 1998; Orgel et al., 2006, 2014; Prockop and Fertala, 1998) (Fig. 5E-I). The intercalation of hydroxyapatite crystals into the collagen fibrils strongly depends on the internal organization of the collagen triple helices (Orgel et al., 2014). Charvolin and Sadoc have suggested a phyllotactic assembly pattern of the collagen triple helices with the in-plane distribution resulting in a sunflower seed type of arrangement (Charvolin and Sadoc, 2011, 2012). Assuming that crystal growth occurs along the path of most adjacent gaps in a fibril, and considering the reported superhelical tilt of the collagen molecules with respect to the fibril axis of about 5° (Hulmes and Miller, 1979), a gently twisted and bent crystal geometry would be in agreement with the experimentally observed crystal morphology in bone (Boyde and Jones, 1998; Landis et al., 1996; Reznikov et al., 2018; Schwarcz et al., 2014). Mineral structure has recently been visualized by scanning transmission electron microscopy (STEM) tomography which has allowed for 3D reconstructions of mineral organization at the nanoscale level – within the tesselle and at the level of individual mineralized collagen fibrils. This method reveals confluent aggregates of crystallites where it is difficult to state whether they are needles or platelets, intrafibrillar or extrafibrillar, and where one crystallite ends and another one starts (Reznikov et al., 2018). It is known that in pristine bone, mineral crystallites would be flexible (Boyde and Jones, 1998). Specifically for this graphic review, we processed previously acquired STEM data (Reznikov et al., 2018) using deep learning-assisted segmentation and applied a watershed transform operation to digitally separate confluent mineral aggregates. Fig. 6 shows the full tomogram with the crystallites volume-rendered and color-coded according to their computationally separable boundaries (which don't necessarily coincide with the elusive true boundaries). Panel B in Fig. 6 shows a few selected aggregates with the modal size varying between 10^5 nm^3 to 10^6 nm^3. This range of volumes would correspond to roughly about 10 to 100 canonically described irregular mineral platelets 10 × 25 × 50 nm (Robinson, 1952). In Fig. 6C, 20 selected individual grains/aggregates are shown with orientation different from that *in situ*, ordered from the largest to the smallest. Despite the remarkable variety of these shapes, the clear common features are that each aggregate (even the smallest one) is a hierarchical assembly on its own (needles fusing into platelets, and platelets stacking into "decks"), and that they are gently curved, resembling fan blades, consistent with prior studies (Boyde and Jones, 1998; Schwarcz et al., 2014), while yet displaying crystalline order at the scale of individual needles (Fig. 7). Interestingly, the larger labels in Fig. 6C appear to recapitulate the curvature that is seen at the edge of a larger tesselle, of which they are indeed a component. Perhaps we should hesitate using comfortable and simplistic depictions of bone's apatite crystallites as being parallelepipeds – they are anything but parallelepipeds – because this description is as accurate as depicting trees like neat cylinders.

In summary, the twisting motif can be found in the skeleton at essentially every magnification level (Zhou, 2021), see also Fig. 8. Although twisted elements of some bones are not always obvious to the unaided eye or through 2D imaging, recent 3D investigations demonstrate how twisting across the nano- and microscales, distinctly among both inorganic and organic constituents, is largely conserved in lamellar bone – whether macroscopically arranged into short, flat, or long bones. At each individual level, twisting within bone's hierarchy appears to enhance bone's overall resistance to biomechanical challenges. This could occur through the twisting of braided collagen fibril bundles into

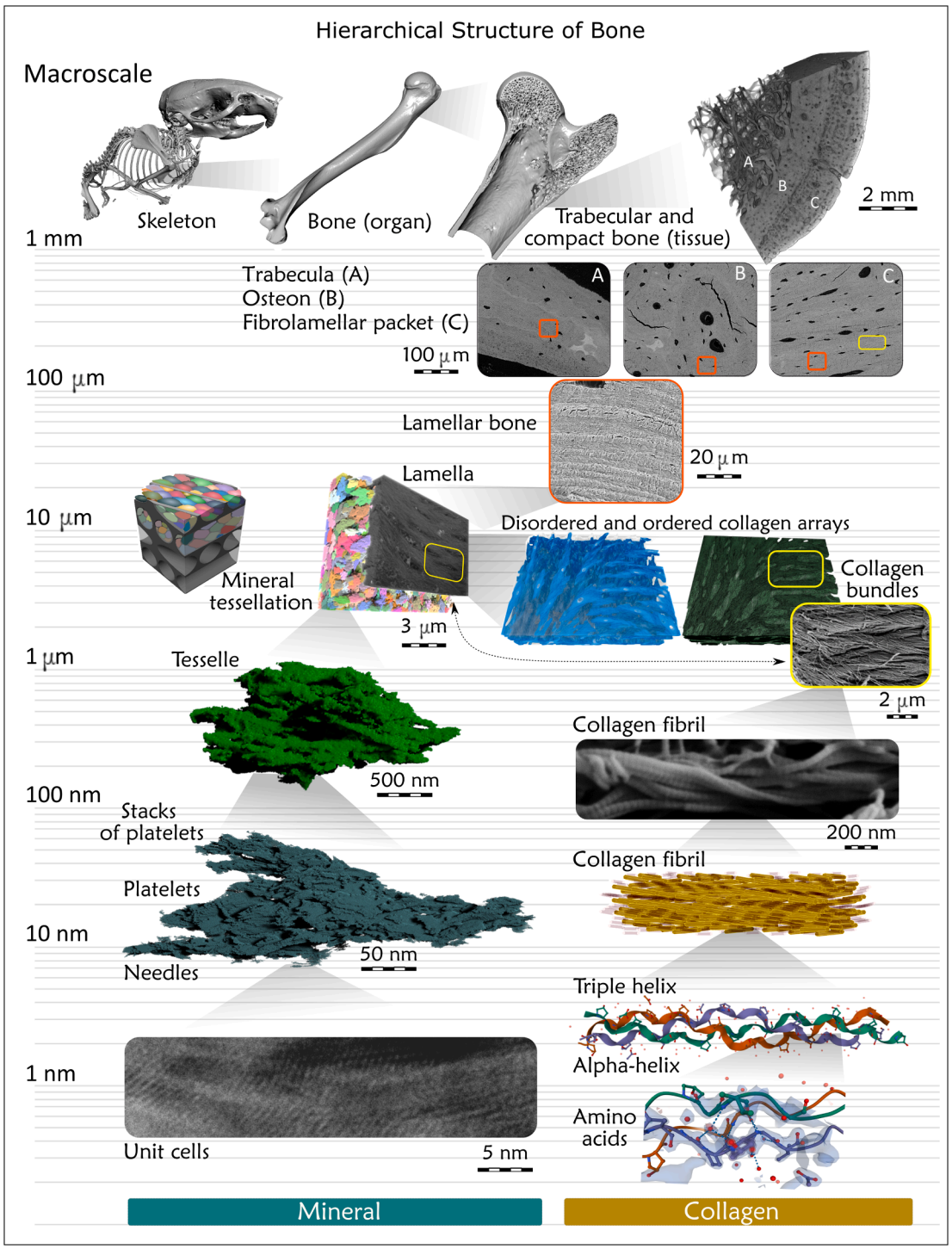

Fig. 8. Contemporary understanding of the hierarchical structure of bone. According to the recent inventory, there are approximately twelve levels: 1) skeletons, made of 2) bones, made of 3) cortical and trabecular tissue, made of 4) cortical osteons, fibrolamellar bone packets, and trabecular lamellar packets, all of which contain 5) lamellar bone, made of 6) lamellae, made of 7) ordered collagen motifs that form 8) bundles, surrounded by the disordered collagen motif. The bundles are made of 9) collagen fibrils, made of 10) triple helices, made of 11) alpha-helices, made of 12) amino acids. The mineral organization in 3D shows its own hierarchical organization starting at level 8) of mineralized collagen bundles, that contain 9) tessellated prolate ellipsoids of mineral, made of 10) mineral platelets, made of 11) laterally merging acicular crystals, made of 12) unit cells. Because the cascade of hierarchical levels splits at the micrometer level for organic and inorganic matter, and because same-level mineral and collagen units have different shapes and even scale (for example, the tesselles, and the collagen fibrils, which are both level 9), and also for visual flow and continuity between levels, we intentionally did not number the levels in the figure.

lamellae that then twist around each osteonal canal, or through the fusion of slightly curved confluent crystal aggregates into spiraling, closely packed mineral tesselles, or through spiraling of trabecular elements at the proximal metaphyses. Maybe this motif occurs for a biomechanical reason – as if the system is thought of as a whole, where springs coil into springs that are coiled into larger springs (and so on) throughout bone's complete hierarchy – in principle, such an assembly could be very resilient indeed (Wagermaier et al., 2006). Comprehensive

simulation studies would be of great value to rule out whether the multiscale "twist of twists" could be a spandrel – being just "the way things are" (Gould and Lewontin, 1979) – or rather (more likely) be there for a reason. Perhaps, twisting might be a truly intrinsic and wide-ranging design principle for hierarchy in Nature's structures (as it appears to be in bone). While exceptions might exist to these notions, it remains an unresolved question in this context as to why a flamingo's or a stilt's legs are so impeccably straight – at least macroscopically!

Declaration of Competing Interest

The authors declare that they have no competing financial interests or personal relationships that could appear to have influenced the work reported in this paper.

Acknowledgements

The authors gratefully acknowledge Jan Dewanckele, TESCAN, for sharing the scans of the mature and juvenile sheep femora acquired in 5 stitched sub-scans at 24 μm and 21 μm voxel size, respectively, and the squirrel humerus, on TESCAN UniTOM XL (Ghent, Belgium). The authors also gratefully acknowledge Hila Tzipora Chase at the UM Flight Lab in Montana for sharing the scan of a humerus of Chukar Partridge (Alectoris chukar) from the Burke Museum collection, acquired at 15 μm voxel size at the Karen F. Liem Imaging Facility of Friday Harbor Labs (Washington, USA). The authors thank Objects Research Systems Inc. (Montreal, Canada), for the free-of-charge academic license for using the Dragonfly™ software. The authors also thank the developers of Inkscape open source software (https://inkscape.org). From McGill University, the authors thank Dr. Kelly Sears and Ms. Weawkamol Leelapornpisit of the Facility for Electron Microscopy Research for assistance with the FIB-SEM work, and Dr. Rui Tahara of the Integrated Qualitative Biology Initiative for assistance with the μCT work. This work was supported by the Canadian Institutes of Health Research (CIHR), and the Canada Research Chairs program (MDM is the Canada Research Chair in Biomineralization). NR and MDM are members of the Quebec Network for Oral and Bone Health Research funded in part by the Fonds de Recherche du Québec – Santé (FRQ-S).

References

Ayoubi, M., Tol, A.F., Weinkamer, R., Roschger, P., Brugger, P.C., Berzlanovich, A., Bertinetti, L., Roschger, A., Fratzl, P., 2021. 3D interrelationship between osteocyte network and forming mineral during human bone remodeling. Adv. Healthcare Mater. 10 (12), 2100113. https://doi.org/10.1002/adhm.v10.1210.1002/adhm.202100113.

Bella, J., Eaton, M., Brodsky, B., Berman, H.M., 1994. Crystal and molecular structure of a collagen-like peptide at 1.9 A resolution. Science 266, 75–81. https://doi.org/10.1126/science.7695699.

Binkley, D.M., Deering, J., Yuan, H., Gourrier, A., Grandfield, K., 2020. Ellipsoidal mesoscale mineralization pattern in human cortical bone revealed in 3D by plasma focused ion beam serial sectioning. J. Struct. Biol. 212 https://doi.org/10.1016/j.jsb.2020.107615.

Boyde, A., Hobdell, M.H., 1968. Scanning electron microscopy of lamellar bone. Z. Zellforsch. 93 (2), 213–231.

Boyde, A., Jones, S., 1998. Aspects of anatomy and development of bone. The nm, um and mm hierarchy. Adv. Organ Biol. 5A, 3–44.

Buss, D.J., Reznikov, N., McKee, M.D., 2020. Crossfibrillar mineral tessellation in normal and Hyp mouse bone as revealed by 3D FIB-SEM microscopy. J. Struct. Biol. 212 (2), 107603. https://doi.org/10.1016/j.jsb:2020.107603.

Charvolin, J., Sadoc, J.F., 2011. A phyllotactic approach to the structure of collagen fibrils. Biophys. Rev. Lett. 06, 13–27. https://doi.org/10.1142/S1793048011001245.

Charvolin, J., Sadoc, J.-F., 2012. About collagen, a tribute to Yves Bouligand. *Interface.* Focus 2 (5), 567–574.

Cook, T.A. The Curves of Life Being an Account of Spiral Formations and Their Application to Growth in Nature, to Science and to Art, With Special Reference to the Manuscripts of Leonardo Da Vinci. (Constable and Company Ltd., 1914).

Currey, J.D., 2003. The many adaptations of bone. J. Biomech. 36 (10), 1487–1495.

Currey, J.D., Shahar, R., 2013. Cavities in the compact bone in tetrapods and fish and their effects on mechanical properties. J. Struct. Biol. 183, 107–122.

Gambaryan, P.P., Kielan-Jaworowska, Z., 1997. Sprawling versus parasagittal stance in multituberculate mammals. Acta Palaeontol. Pol. 42, 13–44.

Gardner, D., 2017. James Bell Pettigrew (1832–1908) MD, LLD, FRS, comparative anatomist, physiologist and aerobiologist. J. Med. Biography 25 (3), 169–178. https://doi.org/10.1177/0967772015605238.

Gebhardt, W., 1906. Ueber funktionell wichtige Anordnungsweisen der feineren und grosseren Bauelemente des Wirbeltierknochens. II. Spezieller Teil Der Bau der Haversschen Lamellensysteme und seine funktionelle Bedeutung. Arch. Entwickl. Mech. Org. 20, 187–322.

Giraud-Guille, M.-M., 1992. Liquid crystallinity in condensed type I collagen solutions. A clue to the packing of collagen in extracellular matrices. J. Mol. Biol. 224 (3), 861–873.

Gould, S.J., Lewontin, R.C., 1979. The spandrels of San Marco and the Panglossian paradigm: a critique of the adaptationist programme. Proc. R. Soc. Lond. B Biol. Sci. 205, 581–598.

Hasegawa, T., Yamamoto, T., Hongo, H., Qiu, Z., Abe, M., Kanesaki, T., Tanaka, K., Endo, T., de Freitas, P.H.L., Li, M., Amizuka, N., 2018. Three-dimensional ultrastructure of osteocytes assessed by focused ion beam-scanning electron microscopy (FIB-SEM). Histochem. Cell Biol. 149 (4), 423–432. https://doi.org/10.1007/s00418-018-1645-1.

Heřt, J., Fiala, P., Petrtýl, M., 1994. Osteon orientation of the diaphysis of the long bones in man. Bone 15 (3), 269–277.

Hulmes, D.J.S., Miller, A., 1979. Quasi-hexagonal molecular packing in collagen fibrils. Nature 282 (5741), 878–880.

Kramer, R.Z., Bella, J., Mayville, P., Brodsky, B., Berman, H.M., 1998. Sequence dependent conformational variations of collagen triple-helical structure. Nat. Struct. Biol. 6, 454–457. https://doi.org/10.1038/8259.

Landis, W.J., Hodgens, K.J., Arena, J., Song, M.J., McEwen, B.F., 1996. Structural relations between collagen and mineral in bone as determined by high voltage electron microscopic tomography. Microscopy Res. Technique 33 (2), 192–202.

McKee, M.D., Buss, D.J., Reznikov, N., 2021. Mineral tessellation in bone and the *Stenciling Principle* for extracellular matrix mineralization. J. Struct. Biol.

Orgel, J.P.R.O., Irving, T.C., Miller, A., Wess, T.J., 2006. Microfibrillar structure of type I collagen in situ. PNAS 103 (24), 9001–9005.

Orgel, J.P.R.O., Persikov, A.V., Antipova, O., Stultz, C.M., 2014. Variation in the helical structure of native collagen. PLoS ONE 9 (2), e89519. https://doi.org/10.1371/journal.pone.0089519.

Pettigrew, J.B., 1908. Design in nature as illustrated by spiral and other arrangements in the inorganic and organic kingdoms as exemplified in matter, force, life, growth, &c., especially in crystals, plants, and animals. Longman, Green, and co. http://archive.org/details/cu31924024737680/page/n29/mode/2up.

Prockop, D.J., Fertala, A., 1998. The collagen fibril: the almost crystalline structure. J. Struct. Biol. 122 (1-2), 111–118.

Reznikov, N., Almany-Magal, R., Shahar, R., Weiner, S., 2013. Three-dimensional imaging of collagen fibril organization in rat circumferential lamellar bone using a dual beam electron microscope reveals ordered and disordered sub-lamellar structures. Bone 52 (2), 676–683.

Reznikov, N., Bilton, M., Lari, L., Stevens, M.M., Kroeger, R., 2018. Fractal-like hierarchical organization of bone begins at the nanoscale. Science 360, eaao2189. https://doi.org/10.1126/science.aao2189.

Reznikov, N., Buss, D.J., Provencher, B., McKee, M.D., Piché, N., 2020. Deep learning for 3D imaging and image analysis in biomineralization research. J. Struct. Biol. 212 (1), 107598. https://doi.org/10.1016/j.jsb:2020.107598.

Reznikov, N., Chase, H., Brumfeld, V., Shahar, R., Weiner, S., 2015. The 3D Structure of the collagen fibril network in human trabecular bone: relation to trabecular organization. Bone 71, 189–195.

Reznikov, N., Shahar, R., Weiner, S., 2014a. Three-dimensional structure of human lamellar bone: the presence of two different materials and new insights into the hierarchical organization. Bone 59, 93–104.

Reznikov, N., Shahar, R., Weiner, S., 2014b. Bone hierarchical structure in three dimensions. Acta Biomater. 10 (9), 3815–3826.

Robinson, R., 1952. An electron microscope study of the crystalline inorganic component of bone and its relationship to the organic matrix. J. Bone Joint Surg. 34A, 389–434.

Schwarcz, H.P., McNally, E.A., Botton, G.A., 2014. Dark-field transmission electron microscopy of cortical bone reveals details of extrafibrillar crystals. J. Struct. Biol. 188 (3), 240–248.

Sehnal, D., et al., 2021. Mol* Viewer: modern web app for 3D visualization and analysis of large biomolecular structures. Nucl. Acids Res. https://doi.org/10.1093/nar/gkab314.

Stolpe, M., Zimmer, K., 1939. Schwirrflug des Kolibri im Zeitlupenfilm. J. Ornithol. 87 (1), 136–155.

Thompson, D.W., 1942. On Growth and Form, 2nd ed. Cambridge University Press.

Wagermaier, W., Gupta, H.S., Gourrier, A., Burghammer, M., Roschger, P., Fratzl, P., 2006. Spiral twisting of fiber orientation inside bone lamellae. Biointerphases 1 (1), 1–5.

Zhou, C., et al., 2021. Chiral hierarchical structure of bone minerals. Nano Res. https://doi.org/10.1007/s12274-021-3653-z.